International Journal of Pharmaceutics 642 (2023) 123147

Contents lists available at ScienceDirect

International Journal of Pharmaceutics

journal homepage: www.elsevier.com/locate/ijpharm

Poly-ε-caprolactone nanocapsules loaded with copaiba essential oil reduce inflammation and pain in mice

Erveton Pinheiro Pinto [a], Sarah Olivia Alves Mendes da Costa [b], Cecile D'Haese [c], Bernard Nysten [c], Francisco Paiva Machado [d], Leandro Machado Rocha [d], Tiago Marcolino de Souza [e], Ana Beloqui [f], Renes Resende Machado [b], Raquel Silva Araújo [a,1,*]

[a] Universidade Federal do Amapá, Amapá 68903-419, Brazil
[b] Universidade Federal de Minas Gerais, Belo Horizonte 31270-901, Brazil
[c] Université Catholique de Louvain, Institute of Condensed Matter and Nanosciences, Bio & Soft Matter, 1348 Louvain-la-Neuve, Belgium
[d] Universidade Federal Fluminense, Faculdade de Farmácia, Laboratório de Tecnologia de Produtos Naturais, 24241-000 Niterói, Rio de Janeiro, Brazil
[e] Universidade do Estado do Amapá, Amapá 68900-070, Brazil
[f] Université Catholique de Louvain, Louvain Drug Research Institute, Advanced Drug Delivery and Biomaterials, 1200 Brussels, Belgium

ARTICLE INFO

Keywords:
Copaiba
Essential oil
Nanocapsules
Inflammation

ABSTRACT

Diverse drugs have been used for the management of inflammation disorders and pain. However, they present many side effects and stimulate the search for new pharmacotherapeutic alternatives. Plant-derived products such as copaiba essential oil (CO) offer beneficial pharmacological effects. On the other hand, essential oil's low water solubility and physical instability hinder its *in vivo* application. Thus, poly-ε-caprolactone (PCL)-based nanocarriers have been used to increase their stability and efficacy. This work aimed to encapsulate CO in PCL nanocapsules and evaluate their effect on inflammation models and pain. The polymeric nanocapsules loading CO (CO-NC) were prepared by nanoprecipitation technique, characterized, and analyzed for their anti-inflammatory effect *in vitro* and *in vivo*. The results showed that CO-NC presented a spherical shape, 229.3 ± 1.5 nm diameter, and a negative zeta potential (approximately −23 mV). CO and CO-NC presented anti-inflammatory and antioxidant effects by LPS-activated macrophages (J774 cells). In addition, CO-NC significantly reduced TNF-α secretion (3-fold) compared to CO. *In vivo*, pre-treatment with CO or CO-NC (50, 100, 200 mg/kg, intraperitoneal; i.p) reduced the mechanical allodynia, paw edema, and pro-inflammatory cytokines induced by intraplantar (i.pl) injection of carrageenan in mice. Specifically, CO-NC (200 mg/kg; i.p.) reduced the production of TNF-α similar to the control group. Our results support using polymeric nanocapsules for CO delivery in inflammatory conditions.

1. Introduction

Inflammation is an immune system response triggered by harmful stimuli. During acute inflammatory responses, cellular and molecular events efficiently minimize impending injury or infection and contribute to restoring tissue homeostasis. However, this response can progress to a chronic process, contributing to the pathogenesis of several diseases. The inflammatory reaction is recognized by cardinal signs and symptoms, such as redness, swelling, heat, pain, and loss of tissue function (Nathan and Ding, 2010; Chen et al., 2018). Pain is a symptom that leads patients to seek medical care (National Institutes of Health, 2019). The pharmacotherapeutic arsenal used to control the signs and symptoms of inflammation, including pain, comprises non-steroidal anti-inflammatory drugs (NSAIDs), steroidal anti-inflammatory drugs, opioids, antidepressants, and anticonvulsants. Despite being widely used in clinical management, these drugs can induce severe adverse effects such as myocardial infarction, strokes, and gastrointestinal toxicity (Vyvey, 2010; Colloca et al., 2017; Schüchen et al., 2018). Therefore, searching for new pharmacological alternatives for treating patients with inflammatory and painful conditions is necessary.

In this context, natural products are essential for developing new drugs. The Brazilian ecosystem has a diversity of medicinal plants that

* Corresponding author.
E-mail address: raquel.araujo@ufop.edu.br (R.S. Araújo).
[1] Present address: Pharmacy Department, Universidade Federal de Ouro Preto, Campus Morro do Cruzeiro, Ouro Preto, MG 35400-000, Brazil.

https://doi.org/10.1016/j.ijpharm.2023.123147
Received 6 December 2022; Received in revised form 12 June 2023; Accepted 14 June 2023
Available online 17 June 2023

operate as a source of identifying pharmacologically active substances, which may act as an alternative for treating patients with different pathological conditions (Boufridi and Quinn, 2018). Among the plants used by the Brazilian population, the copaiba stands out. Many studies have demonstrated the anti-inflammatory and antinociceptive activities of copaiba oil-resin in different experimental models, including acute inflammation induced by zymosan and LPS (Veiga-Júnior et al., 2007), abdominal writhing induced by acetic acid, formalin test, tail-flick test, and hot plate test (Gomes et al., 2007). More recently, the copaiba essential oil (CO) has been studied as an anti-inflammatory, and suppression of pro-inflammatory cytokines IL-6, IL-1β, and IL-8 were seen in LPS-stimulated RAW 264.7 macrophages. However, its anti-inflammatory effects *in vivo* are lacking. The anti-inflammatory effect is attributed to the presence of sesquiterpenes such as β-caryophyllene, α-copaene, and α-humulene, which were associated with anti-inflammatory activities (Destryana et al., 2014; Dahham et al., 2015; Ames-Sibin et al., 2018; Urasaki et al., 2020a, 2020b). Despite the promising application of CO, essential oils are a mixture of volatile and lipophilic substances that present water insolubility, susceptible to degradation by physical and chemical agents (Flores et al., 2011). Therefore, encapsulating essential oil into polymeric nanocapsules can be an alternative to overcome these inconveniences (Reis et al., 2006a, 2006b; Flores et al., 2011; Fraj et al., 2019; Sánchez-Gómez et al., 2022).

Polymeric nanocapsules (NC) are vesicular nanostructures of an oily core surrounded by a polymeric wall. They have advantages such as controlled drug release and high encapsulation of lipophilic components (Araújo et al., 2019; He et al., 2022; Miceli et al., 2022). Furthermore, nano-scaled particles have been found to accumulate in inflamed regions preferentially (Collnot et al., 2012; Qi et al., 2019; Beloqui et al., 2014; Pereira et al., 2009). Poly-ε-caprolactone (PCL) polymer has been widely used for developing nanocarriers due to its biodegradability, biocompatibility, and controlled drug-release properties as it presents a more extended degradation period than other polyester polymers. In addition, PCL-NC protects the encapsulated agent (Flores et al., 2011). PCL has been formulated as NC-loading hydrophobic components for diverse applications such as inflammation and pain treatments. The anti-inflammatory effects of PCL-NC containing bullfrog oil and sucupira oil were reported in the literature (Amaral-Machado et al., 2021; Miceli et al., 2022). The encapsulation of α-terpineol into PCL-NC prolonged the antihyperalgesic effect of α-terpineol (Gouveia et al., 2022). The encapsulation of CO into PCL-NC was performed by our group and embedded into chitosan films (CSF), demonstrating superior mechanical properties compared to unloaded CSF and presenting antibacterial activity (Pinto et al., 2023). Despite these promising results, there is still a scarcity of data regarding using PCL-NC encapsulating essential oil, especially CO, in the context of inflammation and pain treatment. Considering these promising advantages, the present work reports the production and characterization of NC loaded with CO. Furthermore, we investigated the *in vitro* and *in vivo* effects of CO-NC to evaluate whether it can be a candidate for managing inflammatory diseases and pain conditions.

2. Materials and methods

2.1. Materials

Poly-ε-caprolactone polymer 42,500 Da (PCL), Polysorbate 80 (Tween 80), Sorbitan monooleate (Span 80), β-caryophyllene (BCAR), 3-(4,5-dimethylthiazol-2-yl)-2,5-diphenyltetrazolium bromide (MTT), dimethylsulphoxide (DMSO), Lipopolysaccharide (LPS, E. coli O111: B4), HTAB, *o*-dianisidine, dexamethasone 21-phosphate disodium salt, and λ-carrageenan were acquired from Sigma-Aldrich (BE) and Sigma-Aldrich (Brazil). Roswell Park Memorial Institute (RPMI) 1640 medium, fetal bovine serum (FBS), penicillin–streptomycin (PEST), Hanks balanced salt solution (HBSS), phosphate-buffered saline (DPBS), and trypsin-EDTA (0.05 %) were purchased from GibcoTM (Invitrogen, UK). Acetone was purchased from Vetec (Brazil). Copaiba essential oil (batch: 105, CO, *Copaifera officinalis*, ρ = 0.915 g/ml) was purchased from Ferquima Indústria e Comércio Ltda (Brazil). Medium-chain triglycerides (Mygliol 812N) were supplied from Sasol (Gmbh, Germany). Phenobarbital was purchased from Sanofi Aventis (Brazil). Ketamine and xylazine were purchased from Ceva Sante Animale (Brazil). All mentioned products were used without further purification. Aqueous solutions used in the experiments were produced with ultrapure-grade water. All the other chemicals were of analytical grade.

2.2. Copaifera officinalis essential oil chemical characterization

The chemical characterization of the *Copaifera officinalis* essential oil was characterized by gas chromatography coupled with a mass spectrometer (GC-MS QP2010, Shimadzu) and quantified by gas chromatography with a flame ionization detector (GC-2014, Shimadzu). The gas chromatographic conditions were realized as described by Esteves et al. (2023).

2.3. Nanocapsules preparation

NC were prepared using a similar methodology as previously reported by Araújo et al. (2019). Briefly, the 0.6 % w/v of PCL polymer, 0.37 % w/v of Span 80, and 2.5 % v/v of CO were dissolved in 20 mL of acetone. This mixture was poured into 40 mL of an aqueous solution containing 0.75 % w/v of Tween 80 and kept under stirring for 10 min. The solvents were removed under reduced pressure to a final volume of 20 mL of CO-NC. Blank-NC was prepared similarly; however, miglyol was added instead of CO.

2.4. Particle size distribution and zeta potential of CO-NC

The hydrodynamic diameter and polydispersity (PdI) of NC were determined by dynamic light scattering (DLS) in Zetasizer Nano ZS (Malvern Instruments, UK) equipped with a 10 mW "red" laser (k = 632.8 nm) and 90° fixed angle detector at 25 °C room temperature. The zeta potential (PZ) was measured in the same equipment by electrophoretic mobility. Samples were analyzed after 1:20 dilution in ultrapure water. Values reported are the mean ± standard deviation (SD) of three different batches of each NC formulation.

2.5. Encapsulation efficiency

The efficiency of the process of β-caryophyllene (BCAR) encapsulation in the NC was calculated following Eq. (1), as previously reported (Araújo et al., 2019). BCAR encapsulation efficiency (EE%) represents the weight percentage of feed BCAR that was encapsulated in the process.

$$EE\% = \frac{c^{finalproduct} - c^{ultrafiltrateofthefinalproduct}}{c^{BCARfeeding}} \quad (1)$$

The amount of BCAR not encapsulated and dissolved in the external phase was found in the ultrafiltrate after centrifuging the samples in AMICON device (Microcon, 50 kDa MWCO, Millipore®) at 400 × g for 30 min under tangential flow. The ultrafiltrate (25 μL) was diluted with methanol up to 1 mL, then centrifuged, and the supernatant assayed by HPLC. The total amount of BCAR in the NC suspension was assessed by dissolving 10 μL of NC colloidal suspension in methanol (10 mL), vortex-mixed for 2 min, followed by sonication for 30 min to disrupt the NC and release the BCAR. Afterward, 1 mL was HPLC injected. The analyses were performed in triplicate.

2.6. HPLC instrumentation and chromatographic conditions

To quantify the BCAR present in the CO, we used a HPLC method using a Shimadzu 20A system with an SPD-20A UV detector set at 210

nm. The separation was performed on a C18 column (Nucleodur 100–5 C18 5 Mm (4 mm × 125 mm) under room temperature. The mobile phase was composed of by a mixture of acetonitrile and water (70:30 v/v) (Gaonkar et al., 2016). The system was run in isocratic mode at a 1.2 mL/min flow rate and the injection volume was 10 μL. The retention time of BCAR was approximately 23 min. The assay was linear over the BCAR concentration range of 0.1–100 μg/ml. The limits of detection (LOD) and of quantification (LOQ) of BCAR were 0.03 μg/ml and 0.1 μg/ml, respectively. The coefficients of variation (CV) for intra and inter-assay were within 5 %.

2.7. Morphological analysis by atomic force microscopy (AFM) and transmission electron microscopy (TEM)

A NC sample of 10 μL (diluted 1:20, v/v in ultrapure water) was deposited onto freshly cleaved mica and dried with argon gas. AFM analyses were performed at room temperature on Dimension Icon multimode AFM (Bruker). The images were obtained in tapping mode using soft Tapping® mode AFM probes (RTESPA-150 from Bruker) and commercial Si probes (Nanosensors) with cantilevers having a length of 125 μm, resonance frequencies of 75–98 kHz, spring constants of 3.0–7.1 N/m, and a nominal tip curvature radius range from 5 to 10 nm at a scan rate of 1 Hz. Dimensional analyses were performed using the "section analysis" of WSxM 5.0 software (https://www.wsxm.eu/download.html). The ratios between NC diameter/height (D/h) were calculated from the topographical profile from AFM images.

The morphological analysis was also performed by transmission electron microscopy (TEM; Tecnai G2-12 - FEI SpiritBiotwin 120 kV). For this analysis, the diluted suspension was deposited in support grid and negatively stained with uranyl acetate solution (2 % m/v) for 30 s.

2.8. In vitro experiments

2.8.1. Cell culture

The J774 murine macrophage cell line was kindly donated by Pr. Marie-Paule Mingeot (Université Catholique de Louvain, UCLouvain, BE). The cells were maintained in RPMI medium supplemented with 10 % FBS and 1 % of PEST solution and maintained in an incubator humidified and saturated with 5 % CO_2 at 37 °C in 75 cm^2 flasks (Corning, Lowell, MA, USA).

2.8.2. Cell viability

The cytotoxicity of the formulations was assayed by the MTT method. Briefly, J774 cells were seeded in 96-well plates at a density of 20,000 cells/well for 24 h. Then, the cells were exposed to CO-NC, and the corresponding unloaded formulation at oil concentrations ranging from 3.6 to 1875 μg/mL, which were dispersed in 100 μL of culture medium for 4 h (J774 cells). After the medium was removed, the wells were washed three times with HBSS. Then, 100 μL of medium containing MTT (0.5 mg/mL) was added to each well, and the plate was incubated for 3 h in the dark. After this incubation period, the medium was removed, and formazan crystals were solubilized with dimethyl sulfoxide (100 μL per well). The absorbance was measured at 570 nm with a Microplate Reader Emax (Molecular Devices, USA). Cell viability was expressed in percentage compared to cells incubated without NC. For all experiments, controls were carried out in parallel: cells in complete medium (100 % viability) and cells in complete medium containing 1 % of Triton X-100 (0 % viability). The experiments were performed in quadruplicate and three repetitions. The IC_{50} was calculated using GraphPad Prism® version 5.

2.8.3. Inhibition of TNF-α production from J774 macrophages

Macrophages were seeded at 100,000 cells/well in 12-well plates and allowed to adhere for 24 h. The cells were exposed for 4 h to the following formulations: (a) Blank-NC (40 μg/ml), (b) CO-NC (20 μg/ml), (c) CO (123 μg/ml). The concentration values were based on the cell viability studies (Section 2.8.2). After this period, the medium was replaced with a fresh medium supplemented with 0.1 μg/ml of LPS to activate the macrophages. Cell-free supernatants were harvested 24 h later and stored at −20 °C for cytokine quantitation. TNF-α was assayed using a mouse TNF-α uncoated ELISA Kit (Thermofischer, Invitrogen Corporation, UK). The absence of cytotoxicity of the different formulations on macrophages was also assessed by MTT.

2.8.4. Quantification of reactive oxygen species (ROS) production

J774 cells were seeded overnight at 25,000 cells/well in the dark using clear bottom 96-well plates. Intracellular levels of ROS were measured using 200 μL of 1 mM solution of 2,7-dichlorofluorescein diacetate (DCFH-DA) reagent for 40 min at 37 °C. Cells were washed with DPBS and incubated for 4 h with 100 μL of Blank-NC, CO-NC or CO dispersed in a culture medium, preserved from light. Cells were then washed once and 100 μL of a 0.03 % v/v hydrogen peroxide solution in DPBS was added. The microplate was incubated for 30 min at 37 °C in the dark at room temperature. The same non-cytotoxic concentrations are used in Section 2.8.3 were selected for this study. Fluorescence intensity was measured with an excitation wavelength of 485 nm and an emission wavelength of 535 nm (Spectrophotometer SpectraMax M2e & program SoftMax Pro, Molecular Devices, LLC, USA). Data are expressed as the intracellular percentage of ROS compared with oxidized control cells (H_2O_2-activated untreated cells).

2.9. In vivo study design and anti-inflammatory effect

2.9.1. Animals

Female Swiss mice (25–30 g) were used in this study. The animals were acclimatized to a room with a 12 light–dark cycle for at least three days before the experiment. A room temperature of 27 °C, corresponding to the thermoneutral zone for mice was used. The study was approved by the Ethics Committee on Animal Experimentation of the Federal University of Minas Gerais (Protocol 125/2021) and carried out according to the ethical guidelines for the investigation of experimental pain in conscious animals (Zimmermann, 1983).

2.9.2. Mechanical allodynia induced by carrageenan

Mechanical allodynia was measured using an electronic von Frey apparatus (Model EFF 301, Insight, Brazil) as previously described (Melo et al. 2019). After acclimatization of the animals to the experimental apparatus (1 h/day for 3 days), the baseline paw withdrawal threshold (PWT; mean of three measurements) of each animal was determined and expressed in grams. The division of the ten (10) groups for further treatment was done so that the mean baseline PWTs of the different experimental groups were similar. On the experimental day, carrageenan (600 μg, 30 μL) (group 2) was injected via the intraplantar (i.pl.) 30 min after i.p. administration of the vehicle (Tween-80 1 %, 10 mL/kg, i.p) (group (1) CO-NC (50, 100 or 200 mg/kg) (groups 3,4 and 5), CO (50, 100 or 200 mg/kg) (group 6, 7, and 8), Blank-NC (group 9), or dexamethasone (2 mg/kg) (group 10). 200 mg/ml of CO and its equivalent amount in CO-NC was selected for the experiments. The PWT of each animal was measured at 2, 4, 6, 24, and 48 h after carrageenan injection.

2.9.3. Evaluation of motor coordination

The motor coordination of the animals was evaluated on the rota-rod apparatus as described by Morais et al. (2018). The animals were trained on the apparatus for three days before the experiment. On the experimental day, the mice were placed on the rota-rod (14 rpm) and the time (s) they spent on it was measured. The cut-off time was 120 s. After determination of the baseline values, vehicle (Tween-80 1 %, 10 mL/kg, i.p) (group (1), CO-NC (200 mg/kg) (group 2), CO (200 mg/kg) (group 3), Blank-NC (group 4), phenobarbital (50 mg/kg) (group 5) was administered. The animals were tested in the apparatus 0.5, 2, 4, and 6 h later. Results were expressed as time (s) spent on the rotating rod.

2.9.4. Paw edema induced by carrageenan

Paw edema was measured with a plethysmometer (Model 7140, Ugo Basile, Italy). The baseline volume of the right hind paw was measured. Next, the animals were divided into the experimental groups in such a way that the mean paw volumes of the different groups were similar. On the experimental day, carrageenan (600 μg, 30 μL) (group 2) was injected via the intraplantar (i.pl.) 30 min after i.p. administration of vehicle (Tween-80 1 %, 10 mL/kg, i.p) (group (1) of CO-NC (50,100 or 200 mg/kg) (groups 3,4 and 5), CO (50,100 or 200 mg/kg) (group 6, 7, and 8), Blank-NC (group 9) or dexamethasone (2 mg/kg) (group 10). The paw volume of each animal was again measured at 2, 4, 6, 24 and 48 h after injection of the inflammatory stimulus. The results were expressed as the paw volume change (μL) in relation to the baseline values.

2.9.5. Tumor necrosis factor-α (TNF-α), interleukin-1β (IL-1β), and interleukin-6 (IL-6) concentrations in the paw tissue

Carrageenan (600 μg, 30 μL) (group 2) was injected via the i.pl. 30 min after i.p. administration of vehicle (Tween-80 1 %, 10 mL/kg, i.p) (group (1), CO-NC (200 mg/kg) (group 3), CO (200 mg/kg) (group 4) or Blank-NC (group 5). The animals were anesthetized with a mixture of ketamine and xylazine (90/9 mg/kg, i.p.) and euthanized by cervical dislocation 4 h after carrageenan injection and the paw tissue was removed and processed as described by Costa et al. (2022). TNF-α, IL-1β, and IL-6 concentrations were measured in the ipsilateral footpad tissue using ELISA assays, following the instructions supplied by the manufacturer (DuoSet kits, R&D Systems, Minneapolis, USA). All samples were assayed in duplicate, and the results were expressed as pg/100 mg of tissue.

2.10. Statistical analysis

The results were presented as mean ± standard error of the mean (S.E.M.). Both temporal changes and areas under curves (AUC) were shown. AUC was calculated using the trapezoidal rule with the aid of GraphPrism 5.0 for Windows software. Differences were evaluated by using one-way or two-way ANOVA followed by Newman-Keuls or Bonferroni post-hoc. A $p < 0.05$ was considered significant. Statistical analysis was conducted using GraphPrism 5.0 for Windows software.

3. Results

3.1. Characterization

3.1.1. CO and nanocapsules characterization

In this work, the CO essential oil characterization by GC allowed the identification of 90.104 %, showing the sesquiterpenes fraction as the most representative in the oil (89.571 %) (Table 1). The β-caryophyllene (53.5777 %) was the major compound, followed by α-*trans*-bergamotene (9.3057 %) and α-humulene (8.4750 %). Corroborating the previous results, CO presented 55.3 ± 2.3 % of BCAR quantified by HPLC. Pinto et al. (2023) and Monteschio et al. (2021) also found that BCAR represents more than 50 % of CO. The particle characterization of Blank-NC and CO-NC is summarized in Table 2. Both NC had an average size below 250 nm, PdI < 0.3, and negative zeta potential. Regarding size and zeta potential, there was a significant difference between Blank-NC and CO-NC values, indicating that these parameters were affected by the type of oil encapsulated. The encapsulation efficiency (% EE) of BCAR in CO-NC was 74.1 ± 6.0 %. The morphology and diameter of the CO-NC were further analyzed by AFM and TEM (Fig. 1). The height and phase images showed a spherical shape for the nanocapsules. Analysis of the topographical profile (Fig. 1E) indicated a particle average diameter and height equal to 198.8 ± 13.1 nm and 18.3 ± 1.3 nm, respectively. The diameter/height ratio of 10.9 ± 0.3 is consistent with a fluid inner core of these NC, as previously reported for other drug-loaded NC studied by our group (Araújo et al., 2015, 2019). TEM images of CO-NC were performed to observe the NC structure and morphology, confirming the spherical shape (Fig. 1D) demonstrated in AFM images.

Table 1
Chemical characterization of essential oil from *Copaifera officinalis* by GC-MS and GC-FID.

	RT	AI_{calc}	AI_{lit}	Substances	%
1	20.201	1337	1335	δ-elemene	0.6973
2	20.712	1349	1348	α-cubebene	0.9516
3	21.811	1375	1374	α-copaene	5.0381
5	22.781	1399	1389	β-elemene	0.3371
6	23.601	1419	1417	β-caryophyllene	53.5777
7	24.185	1433	1434	γ-elemene	0.6778
8	24.275	1435	1432	α-*trans*-bergamotene	9.3057
10	24.981	1453	1452	α-humulene	8.4750
11	25.939	1477	1480	Germacrene D	2.6927
15	26.769	1497	1500	α-muurolene	1.2839
17	27.23	1509	1505	β-bisabolene	3.7843
18	27.433	1514	1513	γ-cadinene	0.2525
19	27.805	1524	1522	δ-cadinene	2.4978
20	30.074	1582	1582	Caryophyllene oxide	0.5331
Total					90.1046
Sesquiterpene hydrocarbons					89.5715
Oxygenated sesquiterpene					0.5331

*RT, retention time; AI_{lit}, arithmetic index from literature; AI_{calc}, arithmetic index calculated.

Table 2
Physicochemical characterization of the nanocapsules.

Sample	Size (nm)	PdI	ZP (mV)	% EE
Blank-NC	238.7 ± 4.4^{b}	0.210 ± 0.036^{a}	-31.0 ± 0.7^{a}	–
CO-NC	229.3 ± 1.5^{a}	0.208 ± 0.010^{a}	-22.8 ± 1.2^{b}	74.1 ± 6.0 %

PdI: polydispersity index; ZP: zeta potential; % EE: encapsulation efficiency; Different letters in the same column indicate a significant difference ($p < 0.05$).

3.2. In vitro anti-inflammatory and antioxidant studies

The MTT test was performed to select the appropriate concentration for cells' anti-inflammatory and oxidative stress studies. The IC_{50} of oil (miglyol or CO) was 57, 80, and 30 μg/ml for Blank-NC, CO, and CO-NC, respectively (Table 3). The inhibition of TNF-α and ROS production was evaluated by comparing the different formulations that were either Blank-NC, CO, or CO-NC (Fig. 2). Both CO-based formulations significantly reduced ROS and TNF-α levels compared to untreated cells and Blank-NC (control). In addition, CO-NC provided higher TNF-α inhibition compared to CO, indicating the higher activity of CO when encapsulated in NC (Fig. 2B) ($p < 0.05$).

3.3. In vivo studies

3.3.1. Effects of CO-NC and CO on the mechanical allodynia induced by carrageenan

PWT was markedly reduced after i.p. injection of carrageenan (baseline = 6.89 ± 0.19 g, 4 h = 2.47 ± 0.17 g; $p < 0.001$) and Blank-NC, used as a control negative (baseline = 6.77 ± 0.25 g, 4 h = 2.98 ± 0,09 g; $p < 0.001$) (Fig. 3A). As can be seen, CO-NC, CO, and dexamethasone significantly reduced the mechanical allodynia when compared to the control. The maximal effects induced by the dexamethasone and the highest dose of CO-NC were similar at all times evaluated (CO-NC 200 mg/kg, 2 h = 5.67 ± 0.33 g, 4 h = 4.97 ± 0.24 g, 6 h = 5.28 ± 0.13 g, 24 h = 5.70 ± 0.20 g, 48 h = 6.07 ± 0,08 g; dexamethasone 2 h = 5.62 ± 0.20 g, 4 h = 5.40 ± 0.26 g, 6 h = 5.72 ± 0.14 g, 24 h = 5.87 ± 0.14 g, 48 h = 6.30 ± 0.19 g; $p < 0.001$).

3.3.2. Effects of CO-NC and CO on the motor coordination

To investigate whether the inhibition of the nociceptive behavior in

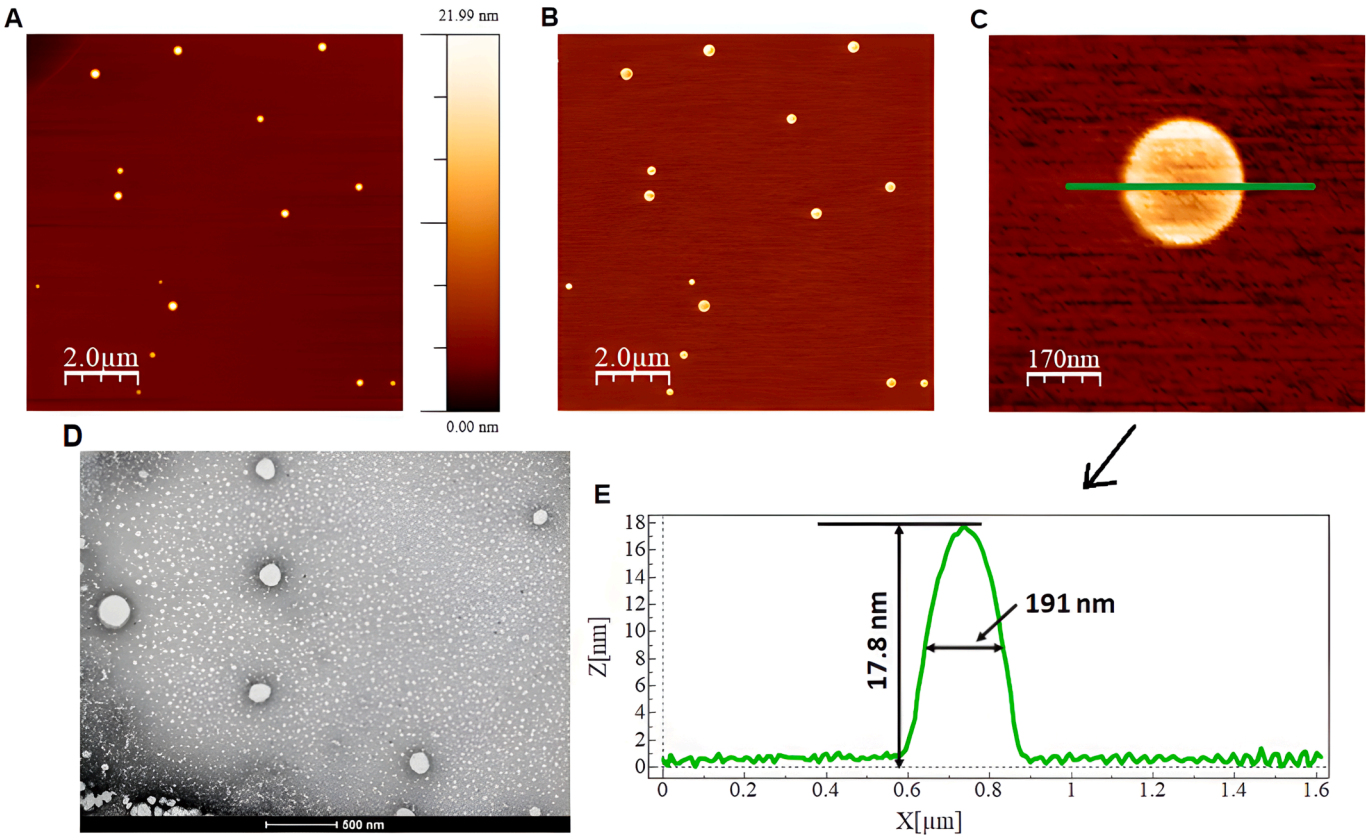

Fig. 1. Atomic force microscopy images of CO-NC. Height image (A) (scan size: 10 μm^2), phase image (B–C) (scan size: 10 μm^2 and 850 nm^2, respectively), TEM photomicrographs (D) and topographical profile (green line) (E) by the "section analysis" of WSxM 5.0 software showing measurements of NC height and diameter in black arrows. The scale bar in (D) equals 500 nm.

Table 3
IC_{50} of Blank-NC, CO and CO-NC on J774 cells.

Formulation	IC_{50} ± SD (µg/ml)
Blank-NC	57.2 ± 0.02
CO	80.1 ± 1.60
CO-NC	30.0 ± 0.06

the animals treated with CO-NC or CO is not the result of motor incoordination, we evaluated its effect on the time spent by the animals on a rotating rod. The time spent was not changed on the rotating rod 0.5, 2, 4, and 6 h after the administration of drugs (Fig. 4). Phenobarbital (50 mg/kg, i.p.) markedly reduced the time mice spent on the rotating rod (0.5 h = 12.33 ± 5.12 s, 2 h = 36.33 ± 12.65 s, 4 h = 44.00 ± 14.79 s, 6 h = 64.33 ± 7.77 s; $p < 0.001$).

3.3.3. *Effect of CO-NC and CO on the paw edema induced by carrageenan*

I.pl. injection of carrageenan (600 µg, 30 µL) induced marked and long-lasting paw edema. All doses of CO-NC (50, 100, 200 mg/kg), as

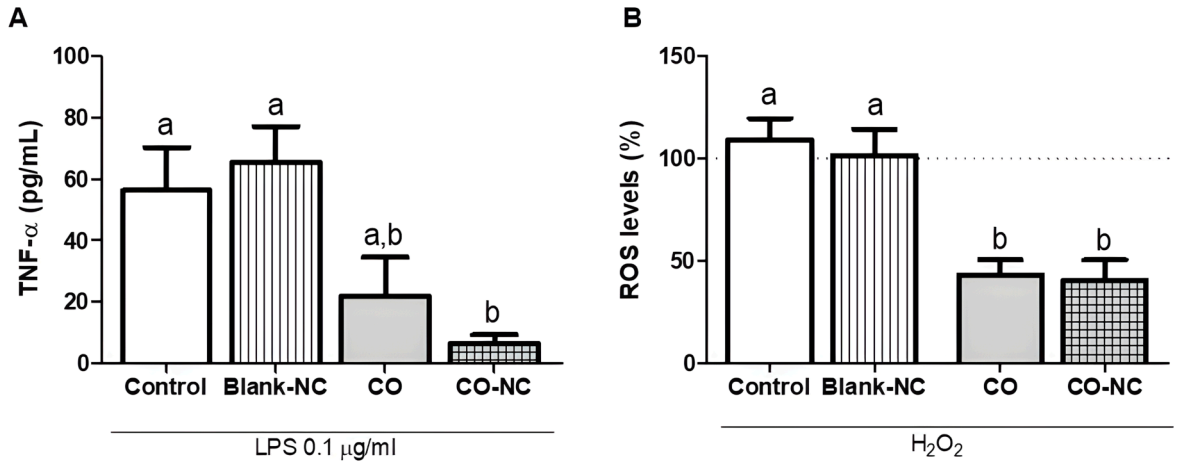

Fig. 2. Evaluation of the anti-inflammatory and antioxidant in LPS-stimulated J774 macrophages. (A) TNF-α quantitation in LPS-activated macrophages. (B) Intracellular ROS quantitation in H_2O_2-stressed macrophages. Data are presented as the mean ± SEM. Different letters indicate statistically significant differences ($P < 0.05$).

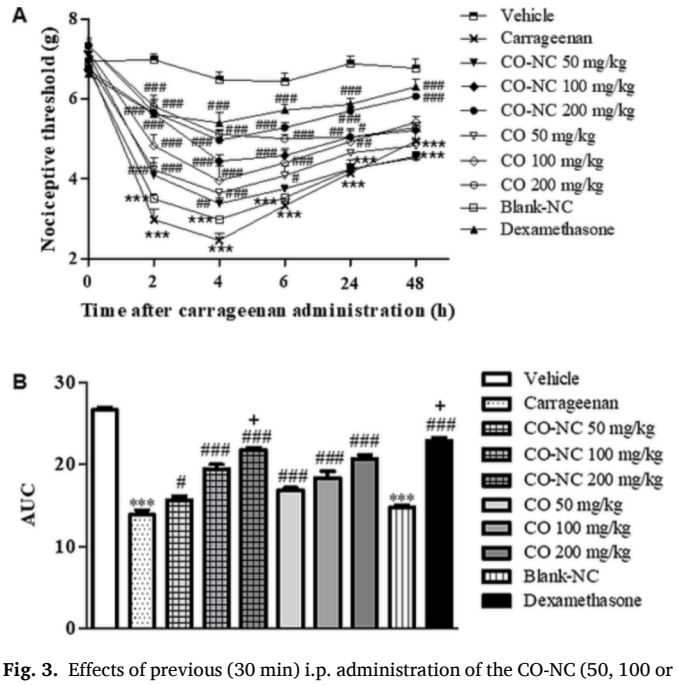

Fig. 3. Effects of previous (30 min) i.p. administration of the CO-NC (50, 100 or 200 mg/kg), CO (50, 100 or 200 mg/kg), dexamethasone (2 mg/kg), Blank-NC or vehicle on the tactile hypersensitivity induced by i.pl. injection of carrageenan (Cg; 600 μg). PWT was evaluated 2, 4, 6, 24, and 48 h after carrageenan injection. Temporal course (A) and AUC (B). ** and *** significantly different from vehicle ($p < 0.01$ and $p < 0.001$, respectively). #, ## and ### significantly different from carrageenan ($p < 0.05$, $p < 0.01$ and $p < 0.001$, respectively). n = 6.

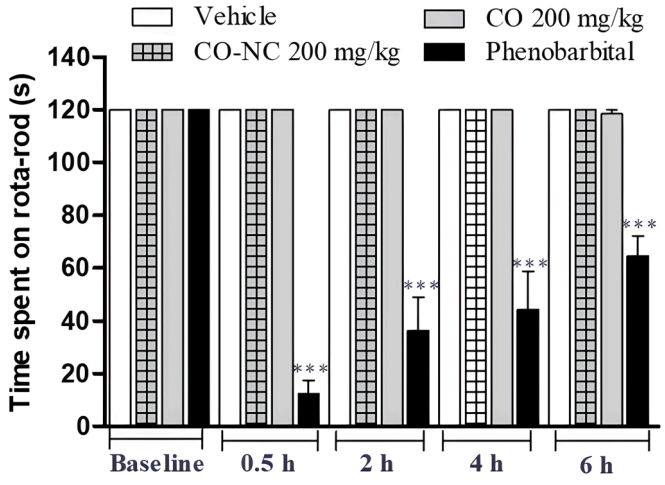

Fig. 4. Effects of previous (30 min) i.p. administration of the CO-NC (200 mg/kg), CO (200 mg/kg), phenobarbital (50 mg/kg), or vehicle on the time spent by mice on the rotating rod. *** significantly different from vehicle ($p < 0.001$). n = 6.

well as the highest doses of CO (100 and 200 mg/kg) and dexamethasone (2 mg/kg), reduced the paw edema induced by carrageenan at all times evaluated (Fig. 5). Blank-NC, as expected, did not present an antiedematogenic effect.

3.3.4. Effects of CO-NC and CO on cytokines production

Four hours after i.pl. injection of carrageenan (600 μg, 30 μL), TNF-α, IL-1β, and IL-6 concentrations in the paw tissue were increased (Fig. 6). Previous (30 min) treatment with CO-NC and CO (200 mg/kg, i.p.) reduced IL-1β and TNF-α levels ($p < 0.0001$). TNF-α concentration was

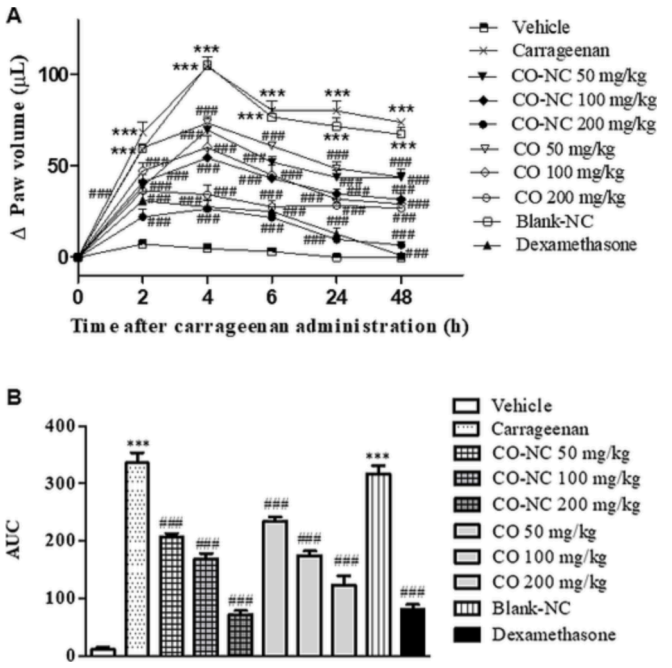

Fig. 5. Effects of previous (30 min) i.p. administration of the CO-NC (50, 100 or 200 mg/kg), CO (50, 100 or 200 mg/kg), dexamethasone (2 mg/kg), Blank-NC or vehicle on the paw edema induced by i.pl. injection of carrageenan (Cg; 600 μg). Paw edema was evaluated 2, 4, 6, 24, and 48 h after carrageenan injection. Temporal course (A) and AUC (B). *** significantly different from vehicle ($p < 0.001$). ### significantly different from carrageenan ($p < 0.001$). n = 6.

reduced only by injection of CO-NC and the concentration of IL-6 was not reduced by any treatment ($p < 0.0001$).

4. Discussion

Nanocarriers have been used to protect the encapsulated active and target inflammation focus (Amaral-Machado et al., 2021; Miceli et al., 2022; Beloqui et al., 2014). The use of bioactive lipids in nanocapsules resides in their documented anti-inflammatory properties (Miceli et al., 2022). Thus, we hypothesized that the association of CO and polymeric NC could increase the anti-inflammatory effects in experimental models of inflammation and pain. The CO chemical composition demonstrated that BCAR is the principal constituent, similar to previous reports for copaiba essential oil (Urasaki et al., 2020; Destryana et al., 2014). The CO-NC obtained by the nanoprecipitation method exhibited a size distribution suitable for parenteral delivery, as they presented a low mean size and a monodisperse population (PdI < 0.30) (Table 2). These nanocapsule properties are in accordance with Pinto et al. (2023), who also encapsulated CO in PCL-NC employing the same nanoprecipitation technique. In addition, CO-NC was produced with PCL, an FDA-approved polymer for internal use and commonly applied for biomedical purposes. Concerning the encapsulation of essential oils, PCL-NC has been demonstrated to protect against volatilization (Flores et al., 2011). Furthermore, Blank-NC and CO-NC formulations exhibited negative zeta potential, which can result from the ionization of chemical groups on the NC surface (such as carboxylic groups of PCL polymer) or ion adsorption. Negative zeta potential values are observed for PCL-NC (Miceli et al., 2022; Pinto et al., 2023). According to the literature, negative charge nanoparticles close to 200 nm can take advantage of greater permeability and retention to accumulate drugs in inflamed tissues (Beloqui et al., 2014; Tirosh et al., 2009). In addition, the smaller the size of the particles, the greater the surface-to-volume ratio they have, which increases their interaction with the cells (Danaei et al., 2018). An encapsulation efficiency (EE) close to 80 % was obtained

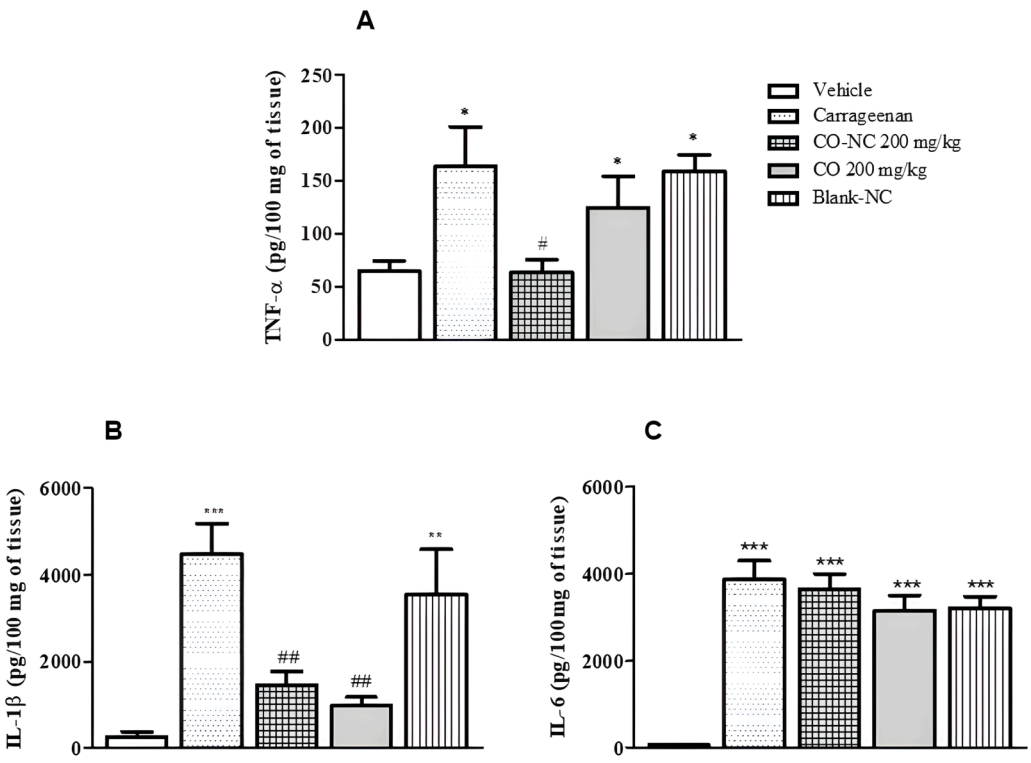

Fig. 6. Effects of previous (30 min) i.p. administration of the CO-NC (200 mg/kg), CO (200 mg/kg), Blank-NC or vehicle on the production of TNF-α (A), IL-1β (B), and IL-6 (C) induced by i.pl. injection of carrageenan (Cg; 600 μg). Cytokine concentrations in the paw tissue were evaluated 4 h after carrageenan injection. *, ** and *** significantly different from vehicle ($p < 0.05$, $p < 0.01$ and $p < 0.001$, respectively). # and ## significantly different from carrageenan ($p < 0.05$ and $p < 0.01$, respectively). $n = 6$.

using BCAR for indirect oil quantification in CO-NC. This result is in accordance with Pinto et al. (2023), who obtained EE close to 74 % for the same formulation, and with Xavier-Junior et al. (2018), who developed chitosan-coated poly(isobutyl cyanoacrylate) nanocapsules loading copaiba oil-resin with EE of approximately 74 %. For other PCL-NC formulations loading copaiba oil-resin and produced by the nanoprecipitation method an EE of 54 % was obtained. However, it was produced at 40 °C (Rodrigues et al., 2023), which can explain the lower EE value compared with the values of this work. EE may be influenced by the production methodology, excipients' chemical nature, and proportions. Different techniques, such as AFM and TEM, have been applied to the study of nanocapsule morphology and dimensions (Abbas et al., 2015; Micelli et al., 2022; Xavier-Junior et al., 2018; Amaral-Machado et al., 2021). Morphological analysis by AFM suggests a spherical shape for CO-NC (Fig. 1) with an average diameter of approximately 199 ± 13 nm. This value is close to the value observed by DLS, 230 nm. In addition, when the phase images represented in Fig. 1B and 1C were analyzed, some phase differences between the NC core and wall confirmed two regions with different viscoelastic properties in the NC (Phani et al., 2021). From the topographic profile in the AFM images (Fig. 1E), the average D/h ratio of CO-NC was close to 11. These results are in accordance with Miceli et al. (2022) and Araújo et al. (2015), who obtained a D/h ratio of approximately 10 and 12 for PCL-NC, respectively. The higher the D/h value, the more flattened the particle. According to the literature, NC deformation can occur due to pressure produced by the tip during AFM analysis but also due to the soft nature of the NC liquid core (Araújo et al., 2015; Araújo et al., 2019; Miceli et al., 2022). This deformation is important since NC should permeate through tissue fenestrations in the body. The TEM photomicrographs (Fig. 1D) show spherical nanocapsules of size and morphology consistent with the results obtained by DLS and AFM, respectively. Furthermore, an electron density difference was observed, indicating the presence of the polymeric wall (Abbas et al., 2015).

During inflammation, nanoparticles are internalized by the immune-related cells. J774 cells are macrophages that produce various inflammatory cytokines. Thus, the anti-inflammatory and antioxidant potential of CO-NC was evaluated in activated murine macrophages (J774 cells). The cytotoxicity of CO and CO-NC was evaluated before determining their activities. CO-NC presented higher toxicity when compared to CO and blank-NC, respectively. This work obtained an IC_{50} of around 80 μg/mL for CO on J774 cells. Destryana et al. (2014) demonstrated an IC_{50} close to 56 μg/mL after 24 h of incubation with *Copaifera reticulata/langsdorfii* essential oil on the macrophage cells RAW 264.7. However, the different copaiba species and macrophage cells could explain the difference found. The results also showed that CO encapsulation into NC increased its activity compared to unloaded CO, similar to Miceli et al. (2022), who encapsulated another oil, SO (sucupira oil), into PCL NC. This suggests that the phagocytic capacity of the cells can be involved as it is known that polymeric NC is actively phagocytized (Araújo et al., 2019).

We found that both CO-formulations exhibited an anti-inflammatory effect, similar to Gelmini et al. (2013), who demonstrated TNF-α, IL-1β, and IL-6 inhibition by copaiba oil-resin in LPS-stimulated monocyte culture (J774 cells). In addition, CO-NC significantly inhibited TNF-α secretion ($p < 0.05$) compared to CO and controls. These results are consistent with those published by Huguet-Casquero et al. (2020), who found that pre-treatment with the polyphenol oleuropein loaded into nanostructured lipid carriers decreased the TNF-α levels after incubation with activated J774 cells. However, in their study, unloaded oleuropein could not exert any effect, contrary to the results shown here. In parallel, CO and CO-NC presented antioxidant activity in activated J774 macrophages. These results demonstrate the *in vitro* potential of CO-NC. Thus, its activity was evaluated in an experimental model of inflammation and pain.

The anti-inflammatory profile is supported by demonstrating CO-NC effects on mice's mechanical allodynia and paw edema induced by carrageenan. Carrageenan is an inflammatory stimulus derived from seaweeds that induces an acute inflammatory reaction after injection, which is characterized by increased vascular permeability, the release of inflammatory mediators such as cytokines, increased sensitivity to thermal and mechanical stimuli, thus contributing to cardinal signs such as edema and allodynia (Necas and Bartosikova, 2013; Gregory et al.,

2013). The highest dose of CO-NC attenuated ongoing mechanical allodynia induced by paclitaxel, similar to dexamethasone, a steroidal anti-inflammatory drug (Fig. 3), and paw edema (Fig. 5) induced by carrageenan. Although antinociceptive data were similar for unloaded and loaded CO, it can be noted that only CO-NC at 200 mg/kg reduced paw edema, similar to dexamethasone, indicating that encapsulation could increase the CO effect. The activities of CO-NC are similar to those demonstrated by other groups of researchers for formulation containing copaiba oil-resin in models of pain and inflammation. Gomes et al. (2007) demonstrated that copaiba oil-resin presented peripheral and central antinociceptive activities after oral administration of 30–150 mg/kg, probably through opioid receptors. Veiga-Júnior et al. (2007) also reported an inhibition close to 45 % and 70 % of the leukocyte and 73 % of the neutrophil accumulation after oral pre-treatment of 100 mg/kg of *Copaifera multijuga*. Lucca et al. (2018) demonstrated that intraplantar application of the hydrogel containing nano-emulsified copaiba oil-resin attenuated the formalin-induced paw edema in Wistar rats.

The anti-inflammatory effect seen here is probably associated with BCAR as it is the major component of the copaiba essential oil in this study. BCAR is a natural sesquiterpene that occurs in essential oils from several plants. BCAR can act as a CB2 receptor agonist, expressed in many tissues and cells under inflammatory conditions. BCAR attenuated mechanical allodynia and reduced inflammatory responses in experimental models (Klauke et al., 2014). Ames-Sibin et al. (2018) verified the similar anti-inflammatory action of copaiba oil-resin and BCAR on arthritic rats after oral administration of 215 and 430 mg/kg. Dahham et al. (2015) demonstrated that oral administration of BCAR (50 to 200 mg/kg) reduced paw edema in carrageenan-induced inflammation, similar to our results for CO. As the higher doses of CO-NC and CO used in the present study did not significantly modify the time that the animals spent on the rotating rod (Fig. 4), it is unlikely that the reduction in the nociceptive threshold induced by these drugs is due to a motor impairment or muscle relaxation.

To evaluate putative mechanisms mediating the antinociceptive and anti-inflammatory activities of CO-NC, we investigated its effects on inflammatory mediators' production. The inflammatory reaction induced by carrageenan culminates in tissue injury, associated with increased production of histamine, serotonin, bradykinin, and prostaglandins, followed by increased levels of pro-inflammatory cytokines such as TNF-α, IL-1β, and IL-6 (Necas and Bartosikova, 2013). CO-NC significantly reduced TNF-α production (Fig. 6) corroborating this work's *in vitro* data (Fig. 2), indicating that encapsulation can increase the anti-inflammatory effect. Regarding IL-1β production, CO-NC and CO were able to decrease their levels. Studies have shown that copaiba oil-resin reduces the production of these cytokines, mainly in different *in vitro* models compared to *in vivo*. Caputo et al. (2020) demonstrated the reduction of IL-4, IL-5, IL-17, and TNF-α in bronchoalveolar lavage fluid in experimental-induced allergic asthma after oral administration of copaiba-oil resin (50 and 100 mg/kg). These studies are in agreement with the present data, where an effective anti-inflammatory effect of copaiba essential oil was demonstrated for the first time in paw edema induced by carrageenan. To our knowledge, this is the first report of CO-NC anti-inflammatory efficacy in different experimental models of inflammation and pain. Thus, the results of the present study demonstrate that CO-NC exhibits antiallodynic and higher anti-inflammatory effects compared to CO, which may be associated with reduced production of pro-inflammatory cytokines.

5. Conclusion

In this study, nano-encapsulated copaiba essential oil (CO-NC) was successfully produced and exhibited suitable physicochemical characteristics for delivering bioactive lipids in inflamed cells. *In vitro*, the highest TNF-α inhibition was obtained using CO-NC, which exhibited a 4-fold decrease compared to unloaded CO. *In vivo*, only CO-NC decreased TNF-α levels induced by carrageenan. Both CO and CO-NC demonstrated a similar antinociceptive effect. These results suggest that the highest dose of CO encapsulated in NC is effective as an anti-inflammatory and are correlated with reduced production of TNF-α and IL-1β. Therefore, the CO-NC developed presented promising characteristics to treat inflammatory disorders, and further studies are necessary to compare this potential with other nanocarriers and inflammation models.

Funding

This work received financial support from Fundação de Amparo à Pesquisa do Estado do Amapá (FAPEAP) and Conselho Nacional de Desenvolvimento Científico e Tecnológico (CNPq) (310748/2021-6 and EDITAL PRONEM, grant # 95/2018). R. Araújo thanks the financial contribution from Wallonie-Bruxelles International (WBI) through the WBI-World Excellence Scholarship. This work was supported by the F.R.S.-FNRS (convention T.0013.19). We also thank Fundação de Amparo à Pesquisa do Estado de Minas Gerais (FAPEMIG; APQ-03027-18), Coordenação de Aperfeiçoamento de Pessoal de Nível Superior (CAPES; Finance Code 001) for financial support.

CRediT authorship contribution statement

Erveton Pinheiro Pinto: Writing – original draft, Investigation, Data curation, Formal analysis. **Sarah Olivia Alves Mendes da Costa:** Writing – original draft, Methodology, Investigation, Data curation, Formal analysis. **Cecile D'Haese:** Methodology, Data curation. **Bernard Nysten:** Methodology, Data curation. **Francisco Paiva Machado:** Methodology, Data curation. **Leandro Machado Rocha:** Methodology, Data curation. **Tiago Marcolino de Souza:** Supervision. **Ana Beloqui:** Methodology, Resources. **Renes Resende Machado:** Supervision, Methodology, Resources. **Raquel Silva Araújo:** Writing – original draft, Methodology, Supervision, Resources.

Declaration of Competing Interest

The authors declare that they have no known competing financial interests or personal relationships that could have appeared to influence the work reported in this paper.

Data availability

Data will be made available on request.

References

Abbas, S., Karangwa, E., Bashari, M., Hayat, K., Hong, X., Sharif, H.R., Zhang, X., 2015. Fabrication of polymeric nanocapsules from curcumin-loaded nanoemulsion templates by self-assembly. Ultrason. Sonochem. 23, 81–92. https://doi.org/10.1016/j.ultsonch.2014.10.006.

Amaral-Machado, L., Oliveira, W.N., Torres-Rêgo, M., Furtado, A.A., Alencar, É.N., Fernandes-Pedrosa, M.F., Rocha, H.A.O., Egito, E.S.T., 2021. Anti-inflammatory activity of bullfrog oil polymeric nanocapsules: from the design to preclinical trials. Int. J. Nanomed. 16, 7353–7367.

Ames-Sibin, A.P., Barizao, C.L., Castro-Ghizoni, C.V., Silva, F.M.S., Sa-Nakanishi, A.B., Bracht, L., Bersani-Amado, C.A., Marcal-Natali, M.R., Bracht, A., Comar, J.F., 2018. β-Caryophyllene, the major constituent of copaiba oil, reduces systemic inflammation and oxidative stress in arthritic rats. J. Cell. Biochem. 119, 10262–10277. https://doi.org/10.1002/jcb.27369.

Araújo, R.S., Garcia, G.M., Vilela, J.M.C., Andrade, M.S., Oliveira, L.A.M., Kano, E.K., Lange, C.C., Brito, M., Brandao, H.M., Mosqueira, V.C.F., 2019. Cloxacillin benzathine-loaded polymeric nanocapsules: Physicochemical characterization, cell uptake, and intramammary antimicrobial effect. Mater. Sci. Eng. C: Mater. Biol. Appl. 104, 110006. doi: 10.1016/j.msec.2019.110006.

Araújo, R.S., Fuscaldi, L.L., Takenaka, I.K.T.M., Vilela, J.M.C., Andrade, M.S., Mosqueira, V.C.F., Cardoso, V.N., 2015. Characterization and in vivo evaluation of nanocapsules loading ^{99m}Tc-MIBI for intramammary study. J. Radioanal. Nucl. Chem. 303, 2353–2360. https://doi.org/10.1007/s10967-014-3763-0.

Beloqui, A., Coco, R., Memvanga, P.B., Ucakar, B., des Rieux, A., Preat, V., 2014. pH-sensitive nanoparticles for colonic delivery of curcumin in inflammatory bowel disease. Int. J. Pharm. 473, 203–212. https://doi.org/10.1016/j.ijpharm.2014.07.009.

Boufridi, A., Quinn, R.J., 2018. Harnessing the properties of natural products. Annu. Ver. Pharmacol. Toxicol. 58, 451–470. https://doi.org/10.1146/annurev-pharmtox-010716-105029.

Caputo, L.S., Campos, M.I., Dias, H.J., Crotti, A.E.M., Fajardo, J.B., Vanelli, C.P., Presto, A.C.D., Alves, M.S., Aarestrup, F.M., Paula, A.C.C., Silva Filho, A.A., Aarestrup, B.J.V., Pereira Junior, O.S., Corrêa, J.O., 2020. Copaiba oil suppresses inflammation in asthmatic lungs of BALB/c mice induced with ovalbumin. Int. Immunopharmacol. 80, 106177 https://doi.org/10.1016/j.intimp.2019.106177.

Chen, L., Deng, H., Cui, H., Fang, J., Zuo, Z., Deng, J., Li, Y., Wang, X., Zhao, L., 2018. Inflammatory responses and inflammation-associated diseases in organs. Oncotarget 9, 7204–7218. https://doi.org/10.18632/oncotarget.23208.

Collnot, E.-M., Ali, H., Lehr, C.-M., 2012. Nano- and microparticulate drug carriers for targeting of the inflamed intestinal mucosa. J. Control. Release 161, 235–246. https://doi.org/10.1016/j.jconrel.2012.01.028.

Colloca, L., Ludman, T., Bouhassira, D., Baron, R., Dickenson, A.H., Yarnitsky, D., Freeman, R., Truini, A., Attal, N., Finnerup, N.B., Eccleston, C., Kalso, E., Bennett, D. L., Dworkin, R.H., Raja, S.N., 2017. Neuropathic pain. Nat. Ver. Dis. Prim. 3, 1–19. https://doi.org/10.1038/nrdp.2017.2.

Costa, S.O.A.M., Rodrigues, I.B., Braga, A.V., Barbosa, B.C.M., Silva, R.R.L., Rodrigues, F. F., Melo, I.S.F., Morais, M., Castro, B.F.M., Cunha Júnior, A.S., Maltarollo, V.G., Oliveira, R.B., Coelho, M.M., Machado, R.R., 2022. RI75, a curcumin analogue, inhibits tumor necrosis factor-α and interleukin-6 production and exhibits antiallodynic and antiedematogenic activities in mice. Inflammopharmacology 30, 505–515. https://doi.org/10.1007/s10787-021-00913-9.

Dahham, S.S., Tabana, Y.M., Ahamed, M.B.K., Majid, A.M.S.A., 2015. In vivo anti-inflammatory activity of β-caryophyllene, evaluated by molecular imaging. Mol. Med. Chem. 1, e1001 https://doi.org/10.14800/mmc.1001.

Danaei, M., Dehghankhold, M., Ataei, S., Davarani, F.H., Javanmard, R., Dokhani, A., Khorasani, S., Mozafari, M.R., 2018. Impact of particle size and polydispersity index on the clinical applications of lipidic nanocarrier systems. Pharmaceutics 10, 57. https://doi.org/10.3390/pharmaceutics10020057.

Destryana, R.A., Young, D.G., Woolley, C.L., Huang, T.-C., Wu, H.-Y., Shih, W.-L., 2014. Antioxidant and anti-inflammation activities of ocotea, copaiba and blue cypress essential oils *in vitro* and *in vivo*. J. Am. Oil Chem. Soc. 91, 1531–1542. https://doi.org/10.1007/s11746-014-2504-4.

Esteves, R., Apolinário, R., Machado, F., Folly, D., Viana, V., Soares, A., Jumbo, L., Svacina, T., Santos, M., Ricci-Junior, E., Oliveira, E., Feder, D., Rocha, L., 2023. Insecticidal activity evaluation of *Persea venosa* Nees & Mart. essential oil and its nanoemulsion against the cotton stainer bug *Dysdercus peruvianus* (Hemiptera: Pyrrhocoridae) and pollinator bees. Ind. Crop. Prod. 194, 116348 https://doi.org/10.1016/j.indcrop.2023.116348.

Flores, F.C., Ribeiro, R.F., Ourique, A.F., Rolim, C.M.B., Silva, C.B., 2011. Nanostructured systems containing an essential oil- protection against volatilization. Quim Nova 34, 968–972. https://doi.org/10.1590/S0100-40422011000600010.

Fraj, A., Jaâfar, F., Marti, M., Coderch, L., Ladhari, N., 2019. A comparative study of oregano (*Origanum vulgare* L.) essential oil-based polycaprolactone nanocapsules/microspheres: preparation, physicochemical characterization, and storage stability. Ind. Crop. Prod. 140, 111669 https://doi.org/10.1016/j.indcrop.2019.111669.

Gaonkar, R., Yallappa, S., Dhananjaya, B.L., Hegde, G., 2016. Development and validation of reverse phase high performance liquid chromatography for citral analysis from essential oils. J. Chromatogr. B 1036, 50–56. https://doi.org/10.1016/j.jchromb.2016.10.001.

Gelmini, F., Beretta, G., Anselmi, C., Centini, M., Magni, P., Ruscica, M., Cavalchine, A., Facino, R.M., 2013. GC-MS profiling of the phytochemical constituents of the oleoresin from *Copaifera langsdorffii* Desf. and a preliminary *in vivo* evaluation of its antipsoriatic effect. Int. J. Pharm. 440, 170–178. https://doi.org/10.1016/j.ijpharm.2012.08.021.

Gomes, N.M., Rezende, C.M., Fontes, S.P., Matheus, M.E., Fernandes, P.D., 2007. Antinociceptive activity of Amazonian copaiba oils. J. Ethnopharmacol. 109, 486–492. https://doi.org/10.1016/j.jep.2006.08.018.

Gouveia, D.N., Guimarães, A.G., Oliveira, M.A., Rabelo, T.K., Pina, L.T.S., Santos, W.B.R., Almeida, I.K.S., Andrade, A., Serafini, M.R., Lima, S., Araújo, A.A.S., Menezes-Filho, J.E.R., Santos-Miranda, A., Scotti, L., Scotti Coutinho, M.T., Quintans, J.S.S., Capasso, R., Quintans-Júnior, L.J., 2022. Nanoencapsulated α-terpineol attenuates neuropathic pain induced by chemotherapy through calcium channel modulation. Polym. Bull. https://doi.org/10.1007/s00289-022-04161-x.

Gregory, N., Harris, A.L., Robinson, C.R., Dougherty, P.M., Fuchs, P.N., Sluka, K.A., 2013. An overview of animal models of pain: disease models and outcome measures. J. Pain 14, 1255–1269. https://doi.org/10.1016/j.jpain.2013.06.008.

He, S., Meng, Q., Zhong, S., Gao, Y., Cui, X., 2022. Sonochemical fabrication of reduction-responsive alginate-based nanocapsules with folate targeting for drug delivery. Colloids Surf. A: Physicochem. Eng. Asp. 639, 128349 https://doi.org/10.1016/j.colsurfa.2022.128349.

Huguet-Casquero, A., Xu, Y., Gainza, E., Pedraz, J.L., Beloqui, A., 2020. Oral delivery of oleuropein-loaded lipid nanocarriers alleviates inflammation and oxidative stress in acute colitis. Int. J. Pharm. 586, 119515 https://doi.org/10.1016/j.ijpharm.2020.119515.

Klauke, A.-L., Racz, I., Pradier, B., Markert, A., Zimmer, A.M., Gertsch, J., Zimmer, A., 2014. The cannabinoid CB2 receptor-selective phytocannabinoid β-caryophyllene exerts analgesic effects in mouse models of inflammatory and neuropathic pain. Eur. Neuropsychopharmacol. 24, 608–620. https://doi.org/10.1016/j.euroneuro.2013.10.008.

Lucca, L.G., Matos, S.P., Kreutz, T., Teixeira, H.F., Veiga Junior, V.F., Araújo, B.V., Limberger, R.P., Koester, L.S., 2018. Anti-inflammatory effect from a hydrogel containing nanoemulsified copaiba oil (*Copaifera multijuga* Hayne). AAPS PharmSciTech 19, 522–530. https://doi.org/10.1208/s12249-017-0862-6.

Melo, I.S.F., Rodrigues, F.F., Costa, S.O.A.M., Braga, A.V., Morais, M.Í., Vaz, J.A., Neto, L. S., Galvão, I., Modolo, L.V., Amaral, F.A., Oliveira, R.B., Fátima, A., Coelho, M.M., Machado, R.R., 2019. 4-Methylbenzenecarbothioamide, a hydrogen sulfide donor, inhibits tumor necrosis factor-α and CXCL1 production and exhibits activity in models of pain and inflammation. Eur. J. Pharmacol. 856, 172404. doi: 10.1016/j.ejphar.2019.172404.

Miceli, J.F.D., Andrade, M.E.R., Carvalho, P.L.A., Santos, E.A., Oliveira, A.E.M.F.M., Fernandes, C.P., Cruz, R.A.S., Garrett, R., Mosqueira, V.C.F., Cassali, G.D., D'Haese, C., Nysten, B., Leite, J.I.A., Cardoso, V.N., Araújo, R.S., 2022. Lecithin-based nanocapsule loading sucupira *(Pterodon emarginatus*) oil effects in experimental mucositis. Toxicol. Rep. 9, 1537–1547. https://doi.org/10.1016/j.toxrep.2022.07.006.

Monteschio, J.O., de Vargas Junior, F.M., Alves da Silva, A.L., das Chagas, R.A., Fernandes, T., Leonardo, A.P., Kaneko, I.N., de Moraes Pinto, L.A., Guerrero, A., de Melo Filho, A.A., Ferraz, V.P., Fagundes, G.M., Muir, J.P., 2021. Effect of copaiba essential oil (*Copaifera officinalis* L.) as a natural preservative on the oxidation and shelf life of sheep burgers. PLoS ONE 16, e0248499. https://doi.org/10.1371/journal.pone.0248499.

Morais, M.I., Rodrigues, F.F., Costa, S.O.A.M., Goulart, F.A., Costa, F.C., Melo, I.S.F., Augusto, P.S.A., Dutra, M.M.G.B., de Fátima, Â., Coelho, M.M., Machado, R.R., 2018. Nicorandil inhibits mechanical allodynia induced by paclitaxel by activating opioidergic and serotonergic mechanisms. Eur. J. Pharmacol. 824, 108–114. https://doi.org/10.1016/j.ejphar.2018.02.014.

Nathan, C., Ding, A., 2010. Nonresolving inflammation. Cell 140, 871–882. https://doi.org/10.1016/j.cell.2010.02.029.

National Institutes of Health, 2019. Pain. https://www.nccih.nih.gov/health/pain. Accessed on: 20 April 2020.

Necas, J., Bartosikova, L., 2013. Carrageenan: a review. Vet. Med. 58, 187–205. https://doi.org/10.17221/6758-VETMED.

Pereira, M.A., Mosqueira, V.C.F., Carmo, V.A.S., Ferrari, C.S., Reis, E.C.O., Ramaldes, G. A., Cardoso, V.N., 2009. Biodistribution study and identification of inflammatory sites using nanocapsules labeled with ^{99m}Tc-HMPAO. Nucl. Med. Commun. 30, 749–755. https://doi.org/10.1097/mnm.0b013e32832f2b59.

Phani, A., Jung, H.S., Kim, S., 2021. Deconvolution of dissipative pathways for the interpretation of tapping-mode atomic force microscopy from phase-contrast. Commun. Phys. 4 https://doi.org/10.1038/s42005-021-00576-6.

Pinto, E.P., Menezes, R.P., Tavares, W.S., Ferreira, A.M., Sousa, F.F.O., Silva, G.A., Zamora, R.R.M., Araújo, R.S., Souza, T.M., 2023. Copaiba essential oil loaded-nanocapsules film as a potential candidate for treating skin disorders: preparation, characterization, and antibacterial properties. Int. J. Pharm. 633, 122608 https://doi.org/10.1016/j.ijpharm.2023.122608.

Qi, H., Yang, L., Li, X., Sun, X., Zhao, J., Hou, X., Li, Z., Yuan, X., Cuia, Z., Yang, X., 2019. Systemic administration of enzyme-responsive growth factor nanocapsules for promoting bone repair. Biomater. Sci. 7, 1675–1685. https://doi.org/10.1039/c8bm01632a.

Reis, C.P., Neufeld, R.J., Ribeiro, A.J., Veiga, F., 2006a. Nanoencapsulation I. Methods for preparation of drug-loaded polymeric nanoparticles. Nanomedicine 2, 8–21. https://doi.org/10.1016/j.nano.2005.12.003.

Reis, C.P., Neufeld, R.J., Ribeiro, A.J., Veiga, F., 2006b. Nanoencapsulation II. Biomedical applications and current status of peptide and protein nanoparticulate delivery systems. Nanomedicine 2, 53–65. https://doi.org/10.1016/j.nano.2006.04.009.

Rodrigues, V.M., Oliveira, W.N., Pereira, D.T., Alencar, É.N., Porto, D.L., Aragão, C.F.S., Moreira, S.M.G., Rocha, H.A.O., Amaral-Machado, L., Egito, E.S.T., 2023. Copaiba oil-loaded polymeric nanocapsules: production and in vitro biosafety evaluation on lung cells as a pre-formulation step to produce phytotherapeutic medicine. Pharmaceutics 15, 161. https://doi.org/10.3390/pharmaceutics15010161.

Sánchez-Gómez, S., Pagán, R., Pavela, R., Mazzara, E., Spinozzi, E., Marinelli, O., Zeppa, L., Morshedloo, M.R., Maggi, F., Canale, A., Benelli, G., 2022. Lethal and sublethal effects of essential oil-loaded zein nanocapsules on a zoonotic disease vector mosquito, and their non-target impact. Ind. Crop. Prod. 176, 114413 https://doi.org/10.1016/j.indcrop.2021.114413.

Schüchen, R.H., Mücke, M., Marinova, M., Kravchenko, D., Häuser, W., Radbruch, L., Conrad, R., 2018. Systematic review and meta-analysis on non-opioid analgesics in palliative medicine. J. Cachexia. Sarcopenia Muscle 9, 1235–1254. https://doi.org/10.1002/jcsm.12352.

Tirosh, B., Khatib, N., Barenholz, Y., Nissan, A., Rubinstein, A., 2009. Transferrin as a luminal target for negatively charged liposomes in the inflamed colonic mucosa. Mol. Pharm. 6, 1083–1091. https://doi.org/10.1021/mp9000926.

Urasaki, Y., Beaumont, C., Talbot, J.N., Hill, D.K., Le, T.T., 2020a. Akt3 regulates the tissue-specific response to copaiba essential oil. Int. J. Mol. Sci. 21 https://doi.org/10.3390/ijms21082851.

Urasaki, Y., Beaumont, C., Workman, M., Talbot, J.N., Hill, D.K., Le, T.T., 2020b. Fast-acting and receptor-mediated regulation of neuronal signaling pathways by copaiba essential oil. Int. J. Mol. Sci. 21 https://doi.org/10.3390/ijms21072259.

Veiga-Júnior, V.F., Rosa, E.C., Carvalho, M.V., Henriques, M.G.M.O., Pinto, A., 2007. Chemical composition and anti-inflammatory activity of copaiba oils from *Copaifera cearensis* Huber ex Ducke, Copaifera reticulata Ducke and Copaifera multijuga Hayne – a comparative study. J. Ethnopharmacol. 112, 248–254. https://doi.org/10.1016/j.jep.2007.03.005.

Vyvey, M., 2010. Steroids as pain relief adjuvants. Can. Fam. Phys. 56, 1295–1297.
Xavier-Junior, F.H., Egito, E.S.T., Morais, A.R., Alencar, E., Alexandre Maciuk, A., Vauthier, C., 2018. Experimental design approach applied to the development of chitosan coated poly(isobutylcyanoacrylate) nanocapsules encapsulating copaiba oil. Colloids Surf. A: Physicochem. Eng. Asp. 536, 251–258. https://doi.org/10.1016/j.colsurfa.2017.02.055.
Zimmermann, M., 1983. Ethical guidelines for investigations of experimental pain in conscious animals. Pain 16, 109–110. https://doi.org/10.1016/0304-3959(83)90201-4.